Review

Bio-Optical Algorithms for ADEOS-2 GLI

B. Greg MITCHELL* and Mati KAHRU*

Abstract

Empirical bio-optical algorithms developed for GLI are described. These algorithms can be used to retrieve in-water properties from GLI normalized water leaving radiances in temperate Case 1 waters. The OC4 Chl-a algorithm uses the maximum band ratio switching procedure for bands that do not saturate over the ocean. GLI is the only ocean color sensor that has ultra-violet (UV) bands and we developed an experimental red tide UV index for the early detection of dinoflagellate blooms. The red tide index uses the increased absorption of UV light by mycosporine-like amino-acids (MAAs). A special version of the Chl-a algorithm was developed for the Southern Ocean Case 1 waters. The standard algorithms cannot be applied to turbid near-shore waters, e.g. off Korea and Hong Kong where bio-optical characteristics deviate drastically from Case 1 characteristics. Developing new and improved algorithms for Case 2 waters is a major challenge in bio-optical oceanography.

Keywords : GLI bio-optical, remote sensing, chlorophyll-a

1. Introduction

The goal of this paper is to describe the bio-optical in-water algorithms of the GLI (Global Imager) aboard the Advanced Earth Observing Satellite-II (ADEOS-II). Validation of the algorithms using in situ data was presented in Murakami et al.[1]. We developed the algorithms using our large, global bio-optical database that includes data from various regions, such as the California Current, Indian Ocean, sub-tropical Atlantic Ocean, Eastern and Western Pacific, the Sea of Japan, East China Sea, the Southern Ocean. Our bio-optical data set includes spectral reflectance (various channels depending on the instrument), chlorophyll-a concentration (Chl-a, using both fluorometric and HPLC methods) and absorption coefficients for particulate and dissolved material. More than 540 sets of reflectance and Chl-a in non-polar areas and nearly 100 sets from the Southern Ocean were used.

The algorithms described here apply to Case 1 waters[2], i.e. waters whose inherent optical properties can be adequately described by phytoplankton and substances covarying with it. As discussed elsewhere[3)~5)], simple empirical algorithms perform well in Case 1 waters for deriving standard products of Chl-a and K490 but introduce large errors when applied to Case 2 waters. Through our collaboration with the National Fisheries Research Development Institute (NFRDI) in Busan, Korea and the Hong Kong University of Science and Technology (HKUST) we have obtained and processed reflectance, absorption and pigment data from turbid Case 2 waters and we demonstrate the errors resulting from their different bio-optical characteristics. While semianalytic algorithms[6)~8)] are capable of deriving more products, they are also more sensitive to errors in calibration and atmospheric correction procedures, especially at short wavelengths.

2. Bio-Optical Algorithms

2.1 Chlorophyll-a concentration (Chl-a)

Due to the possible saturation of some of the GLI bands we had to select bands of normalized water leaving radiance (Lwn) with no expected saturation problem and avoid the bands of first choice, Lwn490 and Lwn565. Our analysis showed that normalizing to Lwn545 may actually improve Chl-a retrieval compared to normalizing to Lwn565. Based on in situ data we found that when using a single band ratio with Lwn545 the sequence of preference of individual bands was as follows : Lwn490, Lwn460, Lwn443, Lwn520. Due to the saturation we could not use the best performing band ratio Lwn490/Lwn545. Our final selection uses the maximum band ratio (MBR) algorithm that switches between the maximum of Lwn443, Lwn460 and Lwn520 to create a ratio with Lwn 545 (Table 1, Fig. 1A). This MBR algorithm is slightly superior to other band ratio algorithms not using Lwn490. Using satellite-derived Lwn data the use of MBR has additional advantages. Due to problems in removing the effects of absorbing aerosols ocean color sensors often erroneously underestimate Lwn at shorter wavelengths. The underestimation can be severe at 412 nm and shorter bands but is common

(Received August 20, 2008. Accepted November 28, 2008)

* Scripps Institution of Oceanography, UCSD, La Jolla, CA 92093–0218, USA

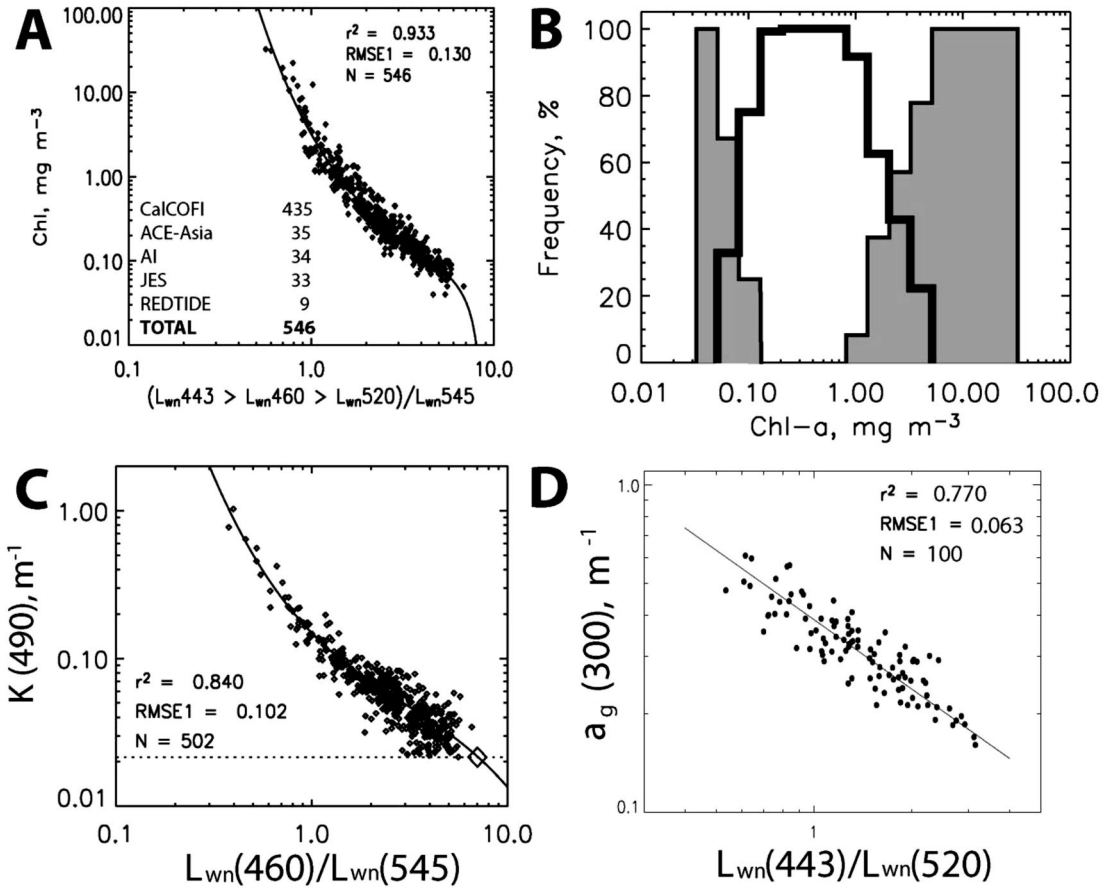

Fig. 1 A, GLI Chl-a algorithm (OC4-GLI) using the maximum band ratio of Lwn443, Lwn460, Lwn520 to Lwn545. Altogether 546 stations with Chl-a and spectral reflectance were used from the following projects : CalCOFI (California Current), ACE-Asia (Central and Western Pacific), AI (Aero-Indo, Atlantic and Indian Oceans), JES (Sea of Japan), REDTIDE (California Current). Only non-polar data were used in developing the algorithm.
B, The selection of the band used in the OC4-GLI maximum band ratio as a function of Chl-a : Lwn443 (14.7%, low Chl-a, left shaded area), Lwn460 (78.7%, middle Chl-a region), Lwn520 (6.6%, high Chl-a, right shaded area). The histograms have been normalized to their maximum value.
C, The GLI K490 algorithm using band ratio of Lwn460 to Lwn545. The pure water value is shown with a horizontal dashed line, the estimated pure water K490 versus Lwn460/Lwn545 is shown as the open diamond.
D, The GLI CDOM algorithm : absorption coefficient at 300 nm as a function of Lwn443/Lwn520.

even at 443 nm[5]. As the MBR algorithm picks the maximum ratio, it will reduce the effects of biased Lwn by switching to longer wavelengths in such cases. The MBR concept was introduced by O'Reilly et al.[4] and applies a single set of coefficients to a band ratio selected as maximum among a set of band ratios. The band actually used in the numerator changes from shorter wavelengths to longer wavelengths with increase in Chl-a. The shortest wavelength band (Lwn443) is typically used at low Chl-a while Lwn460 is used at mid-range and Lwn520 at high Chl-a (Fig. 1B). We modified the MBR scheme by selecting the maximum among the Lwn ratios and not among the remote sensing reflectance (Rrs) ratios. This caused a slight improvement in Chl-a retrieval by a shift towards longer wavelengths.

2.2 Diffuse attenuation at 490 nm (K490)

Due to possible saturation of the GLI 490 nm and 565 nm bands the GLI-K490 algorithm uses is a cubic function of Lwn460/Lwn545 in the log-log space (Table 1, Fig. 1C). In very clear waters the in situ estimate of K490 is close to that of pure seawater. Some of the measured K490 data points in very clear waters were slightly below the pure water value and were excluded when fitting the model equations.

2.3 Colored Dissolved Organic Matter (CDOM)

For the CDOM product all combinations of GLI band ratios were tested versus in situ measurements of absorption coefficient of dissolved material at 300 nm, a_g (300). Several band ratios provided similar values of r^2 and RMS error. The best band ratio with the highest r^2 and lowest RMSE appeared to be Lwn380/Lwn545 (r^2=0.802, RMSE=0.059). Band

Table 1 Formulations of the GLI empirical algorithms.

Variable	Algorithm name	Type	Equation, Coefficients (a), Band Ratio R
CHLA	OC4-GLIv3	Maximum Band Ratio for global Case 1 waters	CHLA = $10^{(a_0 + a_1 \times R + a_2 \times R^2 + a_3 \times R^3) + a_4}$
			$a_{0\text{-}4}$ = [0.531, –3.559, 4.488, –2.169, –0.230]
			R = $\log_{10}$(Lwn443 >Lwn460 >Lwn520) / Lwn545)
CHLA	SPGANT-GLIv3	Maximum Band Ratio for the Southern Ocean	Chl-a = $10^{(a_0 + a_1 \times R + a_2 \times R^2 + a_3 \times R^3) + a_4}$
			$a_{0\text{-}4}$ = [0.573, -2.259, 0.203, -1.300, 0.386]
			R = $\log_{10}$(Lwn443 > Lwn460 > Lwn520) / Lwn545)
K490	GLI-K490	Cubic polynomial in log-log	K490 = $10^{(a_0 + a^1 \times R + a_2 \times R^2 + a_3 \times R^3)}$
			$a_{0\text{-}3}$ = [–0.825, –1.362, 1.094, –0.777]
			R = $\log_{10}$(Lwn460/Lwn545)
CDOM	Kahru and Mitchell, 2001	Linear band ratio in log-log	CDOM300 = $10^{(a_0 + a_1 \times R)}$
			$a_{0,1}$ = [–0.410, –0.703]
			R = $\log_{10}$(Lwn443/Lwn520)
			CDOM440 = $10^{(a_0 + a_1 \times R)}$
			$a_{0,1}$ = [–1.493, –1.618]
Red tide UV index	Kahru and Mitchell, 1998	Threshold of band ratio	REDTIDE index > 0, if R < 0.8 and Chl-a > 1.0
			R = Lwn380/Lwn412

ratios Lwn412/Lwn520, Lwn412/Lwn545 and Lwn443/Lwn 520 were slightly but not significantly inferior. A large proportion of the scatter is actually due to measurement errors and not due to algorithm errors. Atmospheric correction at short wavelengths in the coastal zone is often problematic and may have significant errors. This typically produces under-estimation of the real Lwn[5]. We therefore did not select band ratios including short wavelength bands (380, 412 nm) for the CDOM algorithm. The selected ratio Lwn443/Lwn520 (Table 1, Fig. 1D) appears to be correlated with CDOM absorption due to the fact that a significant part of phytoplankton influence on this ratio tends to cancel out. Additional advantage of this band ratio (compared to band ratios using bands 380 and 400 nm) is that 443 and 520 nm bands are common on other sensors and the same algorithm can therefore be used on these sensors. The operational CDOM definition is the amount of absorption by the dissolved organic component at a certain wavelength, e.g. 300 nm. The CDOM algorithm was developed for a_g(300) but to be compatible with other algorithms we made a version of it for a_g(440). However, as the CDOM signal is much stronger at 300 nm compared to 440 nm, the error of estimating a_g(440) is significantly larger than the error of estimating a_g(300). We therefore recommend using the a_g(300) algorithm.

2.4 Red tide UV index

A novel algorithm for the detection of dinoflagellate blooms (red tides) has been developed using the unique 380 nm spectral band available on GLI that is not available on other past or present ocean color satellites. The algorithm is based on the approach described earlier[9] and should allow the detection of dinoflagellate blooms at relatively low concentrations. Dinoflagellate blooms often grow into red tides. The high absorption in the UV is due to the high intracellular concentrations of mycosporine-like amino acids (MAAs). During and preceding a dinoflagellate red tide the ratio Lwn 380/Lwn412 diverged significantly from the ratio at comparable Chl-a concentrations observed for other periods. The availability of the 380 nm band on GLI allows the potential for red tide detection while concentrations are still moderate. It is critical for this algorithm that the Lwn380 and Lwn412 are accurately derived. This is complicated due to interference by absorbing aerosols and CDOM.

3. Known Problems

3.1 The Southern Ocean Chl-a algorithm

As previously reported[10) 11)], the Southern Ocean has significantly different bio-optical relationships compared to lower

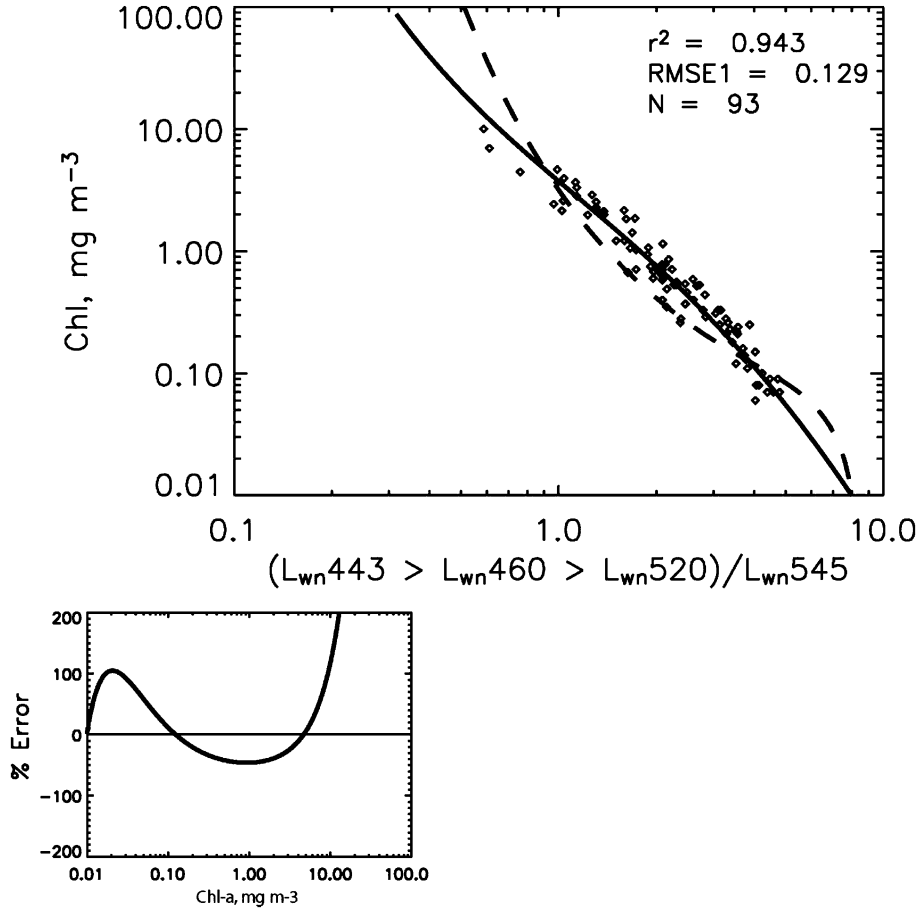

Fig. 2 The Southern Ocean Chl-a algorithm (GLI-ANT) using the maximum band ratio of Lwn443, Lwn460, Lwn 520 to Lwn545 (continuous curve) compared to the standard (non-polar) GLI Chl-a algorithm OC4-GLI (dashed curve). The inset shows the error resulting from using the standard algorithm as a function of Chl-a.

latitudes. Figure 2 shows our Southern Ocean Chl-a algorithm (GLI-ANT), also using the maximum band ratio idea, fitted to our Southern Ocean data sets. Compared to the standard OC4-GLI algorithm GLI-ANT produces significantly higher Chl-a at midrange of Chl-a. Similar discrepancy is observed when using the standard NASA OC4v4 with SeaWiFS wavelengths. The inset of Fig. 2 shows the error of applying the standard algorithm to Southern Ocean data as a function of Chl-a. In the range of 0.2–2.0 mg m^{-3}, the standard algorithms underestimate Chl-a in the Southern Ocean by about 2 times. This is the typical Chl-a range in moderate phytoplankton blooms in the Southern Ocean and therefore important for the accurate detection of primary production and export fluxes in these regions. As confirmed by in situ match-ups in the Southern Ocean[12], standard Chl-a algorithms under-estimate Chl-a in the Chl-a mid-range by 2–3 times. At very high bloom concentrations the relationship is dependent on the phytoplankton type and bio-optical characteristics.

3.2 Problems with Case 2 waters

Creating bio-optical algorithms for turbid waters of East-Asian marginal seas is most challenging. Current bio-optical algorithms and atmospheric correction schemes often produce erroneous results in coastal Case 2 waters. We have assembled a representative bio-optical data set of East-Asian Case 2 waters using data collected by the Hong Kong University of Science and Technology (cruises HK—0007, HK—0102, HK 0103, HK—010426, HK010510) and the Korean National Fisheries Development Institute (cruises NFR0002, NFR 0005, NFR0105, NFR0108). These data sets have been collected by our colleagues using very similar instruments and methods that are identical to ours.

Typical relationships between Chl-a and particulate absorption do not hold in these Case 2 waters (Fig. 3). In Case 1 waters there is a strong relationship between Chl-a and particulate absorption, especially at chlorophyll-a absorption peaks. In the Hong-Kong dataset some data points seem to follow the Case 1 relationship but most do not seem to be correlated with Chl-a at all.

The relationships between Chl-a and CDOM are also quite different : the CDOM concentration in Hong Kong waters is 2–8 times higher than in the California Current at comparable Chl-a concentration (Fig. 4A). However, while the magni-

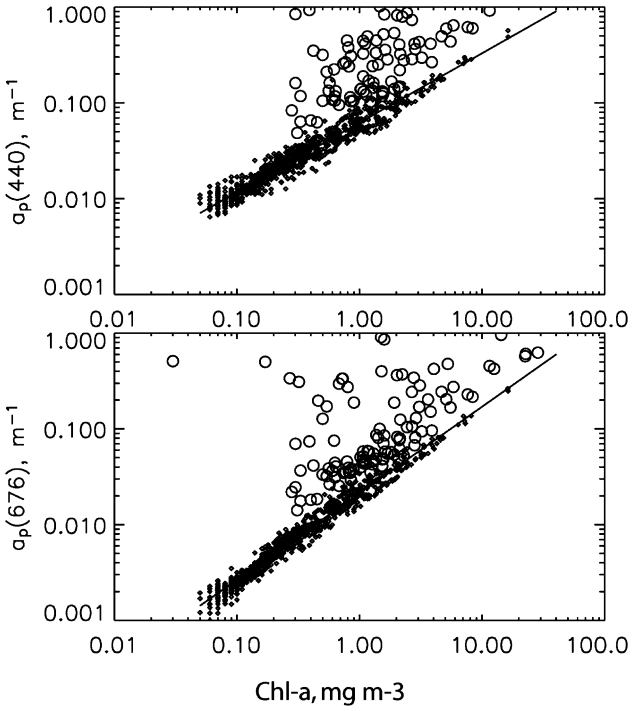

Fig. 3 Coefficient of particulate absorption (a_p) at two Chl-a absorption peaks (440 nm and 676 nm) as a function of Chl-a. The straight line in the log-log space is a typical power-law relationship that holds in Case-1 waters. The data shown as black dots are from the CalCOFI dataset. The open circles are surface data from the Hong Kong coastal waters and show a diversion from the Case-1 relationships.

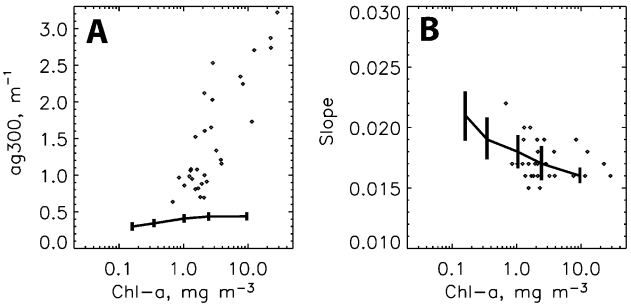

Fig. 4 Absorption coefficient of colored dissolved organic material (CDOM) at 300 nm (a_g 300) and the exponential spectral slope (Slope) as a function of Chl-a concentration in California Current (heavy line) and in Hong Kong (black dots). The relationship in the California Current Case-1 waters shows the median of binned values with the vertical lines showing 1 standard deviation from the median.

tude of CDOM absorFption is much higher, the spectral slope of CDOM absorption is not significantly different from our CalCOFI dataset (Fig. 4B). This seems to indicate that while CDOM concentration is higher, the absorption characteristics are similar to the CDOM in the California Current waters[13].

Due to the drastically increased absorption by particulate and dissolved matter that is weakly or not correlated with Chl-a, it is therefore not surprising that the standard GLI Chl-a algorithm (and other global band-ratio algorithms) cannot retrieve accurate values for Chl-a in turbid Case 2 waters. In most cases the estimated Chl-a values are over-estimated by up to an order of magnitude. It is therefore essential that new approaches are used to develop alternative algorithms for these complex Case-2 waters.

4. Conclusions

Empirical bio-optical algorithm using the maximum band ratio principle developed for GLI retrieves chlorophyll-a concentration for non-polar, Case 1 waters with acceptable accuracy but a modification is needed for the Southern Ocean waters. This algorithm is not acceptable for turbid coastal waters. The empirical algorithms for CDOM and the newly developed red tide UV index for the early detection of dinoflagellate blooms need further validation. Developing new and improved algorithms for Case 2 waters remains a major challenge in bio-optical oceanography.

Acknowledgements

This study was supported by JAXA. The collection of the data sets that made this study possible was funded by NASA through the SIMBIOS project. We thank Prof. Jay-Chung Chen and Wai Man NG of the Hong Kong University of Science and Technology and Dr. Young-Sang Suh of the National Fisheries Research Development Institute (NFRDI), Korea for their in situ data.

References

1) H. Murakami, K. Sasaoka, K. Hosoda, H. Fukushima, M. Toratani, R. Frouin, B. G. Mitchell, M. Kahru, P.-Y. Deschamps, D. Clark, S. Flora, M. Kishino, S.-I. Saitoh, I. Asanuma, A. Tanaka, H. Sasaki, K. Yokouchi, Y. Kiyomoto, H. Saito, C. Dupouy, A. Siripong, S. Matsumura and J. Ishizaka : Validation of ADEOS-2 GLI ocean color products using in-situ observations, J. Oceanogr., 62, 373–393, 2006.

2) A. Morel and Prieur : Analysis of variations in ocean color, Limnol. Oceanogr., 22, 709–722, 1977.

3) B. G. Mitchell and M. Kahru : Algorithms for SeaWiFS

standard products developed with the CalCOFI bio-optical data set, Cal. Coop. Ocean. Fish. Invest. R., 39, 133–147, 1998.
4) J. E. O'Reilly, S. Maritorena, B. G. Mitchell, D. A. Siegel, K. L. Carder, S. A. Garver, M. Kahru, and C. R. McClain : Ocean color chlorophyll algorithms for SeaWiFS, J. Geophys. Res., 103, 24,937–24,953, 1998.
5) M. Kahru and B. G. Mitchell : Empirical chlorophyll algorithm and preliminary SeaWiFS validation for the California Current, Int. J. of Remote Sensing, 20, 3423–3429, 1999.
6) S. A. Garver and D. A. Siegel : Inherent optical property inversion of ocean color spectra and its biogeochemical interpretation. 1. Time series from the Sargasso Sea. J. Geophys. Res., 102, 18,607–18,625, 1997.
7) K. L. Carder, F. R. Chen, Z. P. Lee and S. K. Hawes : Semianalytic Moderate-Resolution Imaging Spectrometer algorithms for chlorophyll a and absorption with bio-optical domains based on nitrate-depletion temperatures, J. Geophys. Res., 104, 5403–5421, 1999.
8) S. Maritorena and D. A. Siegel : Consistent merging of satellite ocean color data using a semi-analytical model. Remote Sensing of the Environment, 94, 429–440.
9) M. Kahru and B. G. Mitchell : Spectral reflectance and absorption of a massive red tide off southern California, J. Geophys. Res., 103, 21,601–21,610, 1998.
10) B. G. Mitchell and O. Holm-Hansen : Bio-optical properties of Antarctic Peninsula waters : Differentiation from temperate ocean models, Deep-Sea Res., 38, 1009–1028, 1991.
11) B. G. Mitchell : Predictive bio-optical relationships for polar oceans and marginal ice zones, J. of Marine Systems, 3, 92–105, 2005, 1992.
12) O. Holm-Hansen, M. Kahru, C. D. Hewes, S. Kawaguchi, T. Kameda, V. A. Sushin, I. Krasovski, J. Priddle, R. Korb, R. P. Hewitt and B. G. Mitchell : Temporal and spatial distribution of chlorophyll-a in surface waters of the Scotia Sea as determined by both shipboard measurements and from satellite data, Deep-Sea Res. II, 51, 1323–1331, 2004.
13) M. Kahru and B. G. Mitchell : Seasonal and non-seasonal variability of satellite-derived chlorophyll and CDOM concentration in the California Current, J. Geophys. Res., 106, 2517–2529, 2001.

● **B. Greg Mitchell**
B. Greg. Mitchell, Research Biologist at UC San Diego, Scripps Institution of Oceanography. Served as NASA Program Manager for Ocean Biogeochemistry 1990–1992. NASA duties included : MODIS Program Scientist 9/1990–3/1991 ; SeaWiFS Program Scientist 10/1990–10/1992. Manager for SeaWiFS Project and Science Team, 1992. Chief Scientist on two interdisciplinary cruises to Southern Drake Passage (2004, 2006). Participant in more than 30 cruises to all oceanic regions.
E-mail : gmitchell@ucsd.edu

● **Mati Kahru**
Mati. Kahru, Project Scientist at UC San Diego, Scripps Institution of Oceanography.